Instrument Science Report HST 2020-03

IR 'Snowball' Occurrences in WFC3/IR: 2009-2019

Joel D. Green
Heather Olszewski

March 31, 2020

ABSTRACT

"Snowballs" are a known IR detector artifact, similar to but distinct from cosmic rays, identified in HST, JWST, Euclid, and WFIRST detectors, that are removed via pipeline processing. Unlike cosmic rays, snowballs generally show a symmetric profile that suggests a local origin from radioactive decay products of the detector itself, rather than a cosmic origin. The snowball occurrence rate, intensity, shape, and variation over time provides important constraints on candidate species by their decay rates, and HST's WFC3/IR has by far the longest time baseline for analysis. We examine WFC3/IR data from June 2014 through December 2019 and identify a conservative and a broader set of criteria to identify snowballs in this dataset. By cross-checking our analysis against datasets from earlier years published in a previous ISR, we find our criteria consistently bracket the previous reported counts, suggesting that the uncertainty in snowball count is captured between our conservative and broader criteria. We report 5261 new snowball detections under the conservative criteria, and 7545 new snowballs under the broader criteria. Added to the 7291 previously identified between 2009 and 2014, this yields a total of 12552 - 14836 snowballs over an 11 year baseline of observations. Given the quantified uncertainties in identification, we find no evidence that the rate of snowball occurrence has changed significantly in WFC3/IR over this period. This constant occurrence rate over the extended time baseline strongly rules out Th-228 radioactive decay as a major contributor. The moderately higher occurrence rate in WFC3/IR compared with most other IR detectors in shielded laboratory environments may suggest the U-238 decay origin as the most likely cause of the snowballs, but does not rule out other effects.

Introduction

"Snowballs" are an identified artifact in HST WFC3/IR data that have also been observed in the IR detectors of JWST/NIRISS, WFIRST, and Euclid. Snowball rates have been measured from 2009 to 2014; except for HST, these snowball counts were measured during laboratory testing. For comparison, normalized to WFC3/IR collecting area, previously published counts include WFC3/IR ($\sim$28.8 per day; Durbin, Bourque, & Baggett, 2015; hereafter D15), JWST/NIRISS ($\sim$ 19.6 per day; Volk 2014), JWST/NIRCam ($\sim$ 4.8 to 14.4 per day; Hilbert 2015) and WFIRST ($\sim$ 9 per day; Cillis et al. 2018), as well as Euclid ($\sim$7-9 per day; Cillis et al. 2018), depositing typically $<10^5$ e^- per event. NIRSpec actually showed a decreasing rate of snowball detections over time (Rauscher et al. 2014). This study predicted that the NIRSpec detector snowball rates would be negligible by 2018, providing an interesting test at the next opportunity. Like cosmic rays, they occur in single reads only and do not significantly affect particular pixels or occur at particular clustered times. Like cosmic rays, their effect on scientific data is mitigated by fitting the slope of the ramp and removing the affected read pixels. As both snowballs and cosmic rays are removed efficiently using the individual reads before being combined (Rajan et al. 2011), it is crucial to note that neither is common enough to significantly affect the final FLT images.

Cosmic ray artifacts are caused by trails of high energy particles impacting the detector, at a rate of $\sim$ 1.20 $s^{-1}cm^{-2}$, with an average deposition per event of 2300 e^- (N. Miles 2020, priv. comm.). Unlike cosmic rays, snowballs deposit relatively large amounts of charge $<10^5$ e^-) and saturate detector pixels in the affected reads. They generally exhibit a close-to-symmetric or elliptical shape, although there are a small number of cases depositing $<10^5$ e^- but with an aspect ratio closer to that of a cosmic ray. The occurrence rate, and the total energy deposited in an event has been used to constrain the possible sources for snowballs. The origin of the snowballs has been variably proposed to be the interaction of the detector material with muons or other high energy particles, or alternately radioactive decay of the detector material itself, via U-234 or U-238, or Th-232 or Th-228. McCullough (2009) show (in their Table 1) that the rate of Th-228 decay should initially decrease and then significantly increase over a ten year period due to the 1.9 yr half-life, while the rate of U-234 decay would be expected to hold steady due to its much longer half-life. Thus if thorium decay is the primary driver of snowballs, the event rate should increase by a factor of 2 to 4, depending on the fraction of events attributed to U-238 decaying to Th-234, over the course of ten years. If muon interactions are the primary driver, then the rate would not change over time, but would be dependent upon the testing site (Hilbert 2009).

WFC3 was installed on HST in 2009, and is now in its eleventh year of activity, providing by far the longest baseline of data to test the snowball occurrence rate. We note that eleven years is actually a lower limit, as the detector was fabricated several years prior to launch in 2009; any decay clock would have started at that time. In this work, we confirm the results of D15 on snowballs in the WFC3 detector from 2009-2014, and analyze five additional years of data through the end of 2019. We consider sources of uncertainty in the classification of snowballs, and compare characteristics to previous studies of snowballs in HST, JWST, and WFIRST. Overall, we find no significant change in the snowball occurrence rate over the eleven year operational period of WFC3/IR, suggesting that if radioactive decay is the source of snowballs, it must be driven by U-238 decay rather than Th-232. Cosmic ray origins (in particular, muons), are not ruled out but are generally not consistent with the observed levels of charge deposited in an event (e.g., Cillis et al. 2018). The consistency of the snowball occurrences rate between the in-flight WFC3 and the test facility based JWST/NIRISS and WFIRST detectors, contained inside varying levels of shielding, may favor the materials decay origin hypothesis.

Criteria for Selecting Snowball Candidates

Our goal was to determine the time-dependent occurrence rate of snowballs, and any direct observational parameters with which they correlate. The identifying criteria for snowballs differ qualitatively between the five analyses considered here (WFIRST: Cillis et al. 2018; JWST/NIRISS: Volk 2014; JWST/NIRCam: Hilbert 2015; WFC3/IR from 2009-2014: D15; WFC3/IR from 2014-2019: this work). In this ISR, we focus primarily on data obtained since the D15 results, from June 2014 to Dec 2019.

Overall, we followed the methodology from D15, previously applied in Hilbert (2009). Candidates were identified using the IR multiaccum ramp, and difference images were generated using successive reads (or frames) in the ramp. Each difference image was searched for pixel(s) more than 50 sigma above background level, collectively to be flagged as a candidate snowball. Beginning with the same automated filtering routines in D15, we searched through all WFC3/IR data in the HST archive, from July 2009 ($\sim$ JD 55028) to Dec 2019 ($\sim$ JD 58823). These programs identified the coordinates in which single-read bursts of flux occurred by looking at the differences between each consecutive set of reads, finding a total of 238931 such occurrences. Secondary routines developed by our team removed numerous false positives, induced by streaks or drift, including observations taken under "Drift-And-SHift" (DASH) mode (Momcheva et al. 2017), and other causes of inter-read drift including guide star acquisition failure. Programs with these issues were removed from the analysis, and the total IR exposure time was reduced accordingly. The remaining snowball candidates totaled 13651 after all automated filtering was completed.

These candidates were grouped by month and ingested into a program used by D15 that facilitated human verification of each individual snowball candidate. The goal of human verification was to verify each candidate snowball, removing by hand flagged detections that are cosmic rays, or misclassifications by the algorithm, caused by edge of the array artifacts, misidentified drifts, or variation of very bright objects near the coordinates. For the human verification phase, our testers agreed upon the following criteria to define snowballs (see Fig. 1 for examples:

1. Does the candidate exhibit a "snowball-like" morphology? In particular, we considered three tests:
   (a) Is the morphology sufficiently symmetric or round to be distinguishable from a cosmic ray? If elongated, are several (> 2) pixels saturated to a level not typical of a cosmic ray?
   (b) Does the candidate show diffraction spikes that would indicate it is a stellar object rather than a snowball?

   (c) Is the morphology distorted by nearby bright sources, edge effects, or other image artifacts that would contaminate the detection?

   (d) Does the snowball occur in only one read?

2. If the candidate's morphology was sufficiently snowball-like, we then used three quantitative diagnostics to discriminate snowball candidates from cosmic rays: total flux, number of pixels ten times above the background level, and number of saturated pixels, consistent with identified radioactive decay effects in HgCdTe arrays (Finger et al. 2008).

   (a) If the candidate's total flux was > 200,000 e^-, and included at least two (central) pixels with flux > 90,000 e^-, and at least 2 saturated pixels, we classified the detection as a "candidate" snowball.

   (b) If the candidate included only one saturated pixel, we considered the distribution of the flux in the central pixels to classify the candidate. If the total flux > 200,000, or at least 2 pixels contained flux > 70,000, or at least 3 pixels contained flux > 50,000, or at least 4 pixels contained flux > 30,000, we classified the detection as a "candidate" snowball.

   (c) In the (rare) case that the candidate exhibited no saturation in any pixels, but total flux > 200,000, and a clear snowball-like morphology as defined in step (1), we classified the detection as a "candidate" snowball.

3. To characterize the uncertainty in human verification, we introduced a new classification, "marginal", indicating candidates that were edge cases, that humans would be classified as snowballs about 50% of the time. This captured a particularly common type of candidate:

   (a) If only one saturated pixel was seen, and the flux threshold defined in step 2 was not reached, we classified the candidate as a "marginal" snowball.

   (b) If no pixels contained flux > 40,000, and no pixels were saturated, we rejected the candidate snowball.

Results

We considered various sources of uncertainty in the verification stage. First, misclassification due to human error (in verifying by eye 13651 snowball candidates) is estimated at 1-2%. We determined this by comparing human verified results from our work with those of D15 for select months, finding occasional cases in which an identified snowball was clearly a cosmic ray or artifact. More rarely, human verification can override the criteria above for a borderline candidate that is sufficiently compelling, but this occurred only in rare circumstances in which an edge effect or variable bright object created a coincidentally snowball-like effect between reads. This was diagnosed by comparing by eye the surrounding reads. However, the overwhelming majority of borderline cases were candidates with snowball-like morphology, but insufficient flux to meet the criteria for "candidate". Our solution was to create the "marginal" category and capture the uncertainty of the faint snowballs. To verify that our human classifiers were calibrated similarly to D15, we conducted double-blind tests on datasets from July 2009 to May 2014, under our new criteria. We thus compared multiple trials under the new criteria to the original snowball list from D15. In all cases, we found that the classifications disagreed between the all three verification trials in about 15-25% of all cases. However, in all tests, the number of snowballs identified in D15 was greater than the number of "candidates" but less than the number of "candidates + marginals" (hereafter referred to as total snowballs) identified under the new criteria. We compared our verification methods with D15 for select months and found that about 50% of "marginals" would be identified as snowballs under their previous criteria (Figure 4). Based on this comparison, we take our overall snowball count to be the "candidates" + half of the "marginals". This is consistent with D15, in which "an effort was made to be conservative with rejections." For completeness, we provide both "candidates" and "marginals" in our snowball atlas update.

For the period June 2014 - Dec 2019, the automated routines returned 13561 snowball candidates. After the verification steps were complete, we found 5261 "candidates" and 2283 "marginals" for a total of 7544 snowballs. The results are currently stored in a single file:

http://www.stsci.edu/files/live/sites/www/files/home/hst/instrumentation/wfc3/...
...documentation/instrument-science-reports-isrs/_documents/snowballs.txt

The overall rate of snowball occurrence over this period (JD 56828 to 58818), normalized to total IR exposure time (20,682,262 seconds or 5745 hours, out of 176,256,000 seconds or 48960 hours over the full time baseline), is 22.0 "candidate" snowballs/day, or 31.5 "candidate + marginal" snowballs/day. Using our overall averaged criteria, we estimate the true snowball rate during 2014-19 as 26.7 ± 4.8 snowballs per day.

Table 1: Comparison of IR snowball studies 2009-2019.

Author	Detector	Array Size	Year(s)	Total Hrs	Rate ($hr^{-1}cm^{-2}$)	Count (10^5e^-)
Cillis+ (2018)	WFIRST	4096×4096	2015-18	348	0.03	1.8 - 4.1
Cillis+ (2018)	Euclid	2048×2048	2015-18	600	0.07	> 1
Durbin+ (D15)	WFC3/IR	1024×1024	2009-14	6200	0.11	∼ 2 - 9
(this work)	WFC3/IR	1024×1024	2014-19	5745	0.1 ± 0.2	∼ 2 - 9
Hilbert (2015)	NIRCam	2048×2048	2014	300	0.03	2.8 - 4.9
Volk (2014)	NIRISS	2048×2048	2014	30	0.08	∼ 1 - 15

Snowball Characteristics and Comparison with D15

The introduction of the "marginal" classification for snowballs allows us to characterize the snowball properties in finer detail. Due to our criteria, the "marginals" are distinguished most strongly by their total flux average and range, and number of saturated pixels, rather than by number of pixels above the background threshold. They are morphologically similar to the typical "candidate", but have much lower flux ($\sim$ 217000 vs. $\sim$ 520000) and many fewer saturated pixels ($\sim$ 2.1 vs. $\sim$ 5.4), but only modestly fewer bright pixels ($\sim$ 12.6 vs. $\sim$ 18.2). There is no statistical difference in the pixel coordinates or read number in which the snowball occurred, and the occurrence positions are distributed in a uniform fashion across the detector. The distributions of both classifications are shown in Figure 2. It appears that the classifications are truncated overlapping distributions, and we hypothesize that the faintest "marginals" and the brightest non-detections are similarly overlapping. We suggest that this zone of uncertainty is reasonably characterized by the second classification bin, similar to the "inconsistent snowballs" classification derived by comparing multiple human verification trials in D15.

The mean snowball flux from 2014 to 2019, presuming that only half of the "marginal" category are snowball detections, is very to the mean snowball flux derived from the 2009 to 2014 data as described in D15, (466000 e^- in this work vs. 504000 e^- in D15).

We find no evidence of any change in snowball properties since the discussion in D15 (Fig 4).The variation in total IR exposure time on a monthly basis (Figure 5, top) fully accounts for the variation in snowball count per month (Figure 5, middle and bottom). The snowball occurrence rate is similar (26.7 in Figure 5 vs. 28.8 in D15), and the snowball distributions are similar (see comparison figure showing distribution snowballs from D15 and current result).

It was suggested in McCullough (2009) that Th-232 daughter decay processes could lead to snowballs recurring in particular pixels up to a day after the initial event. We searched through the snowball database and found only *one instance* in which a snowball occurred three times, within three days, centered within three pixels of the first occurrence centroid. As in D15, we find no evidence of Th-232 daughter decay from temporal or spatial data.

We also examined a handful of the brightest snowballs for evidence of persistence following an event. In this extreme case, the increased count slowly decays in subsequent reads but remains far above background through the full 1400 second integration (Figure 6). Thus we conservatively recommend removing all reads following a snowball occurrence. An in-depth exploration of the effects of snowball occurrences on the affected pixels is beyond the scope of this ISR.

Conclusions

We analyzed WFC3/IR data from June 2014 through December 2019 and identified between 5261 and 7545 new snowball detections. We detailed a cookbook/procedure to identify snowballs and compare more uniformly across datasets and instruments. We found no significant change in the rate of snowball occurrence in WFC3/IR over the 2009-2019 period. This extended time baseline rules out Th-228 decay as a major contributor. WFC3/IR continues to exhibit a moderately higher occurrence rate compared with other IR detectors (JWST, WFIRST, and Euclid) in shielded laboratory environments, suggesting the U-238 decay origin as the most likely cause of the snowballs, but this does not completely rule out the effect of shielding on external triggers including muon or other high energy particle impacts.

Acknowledgements

The authors would like to thank Sylvia Baggett, Nor Pirzkal, Marc Rafelski, Nate Miles, and Norman Grogin for helpful insights in preparing this work.

References

- Cillis, A. et al., 2018, "Snowballs in Euclid and WFIRST Detectors," Proc. SPIE 10698, Space Telescopes and Instrumentation 2018: Optical, Infrared, and Millimeter Wave, 106983A (6 July 2018); doi: 10.1117/12.2312666

- Durbin, M.J., Bourque, M., Baggett, S., 2015, "IR 'Snowballs': Long-Term Characterization", ISR WFC3 2015-01

- Finger, G., Dorn, R.J., Eschbaumer, S., Hall, D.N.B., Mehrgan, L., Meyer, M., & Stegmeier, J., "Performance evaluation, readout modes, and calibration techniques of HgCdTe Hawaii-2RG mosaic arrays", Proc. SPIE 7021, High Energy, Optical, and Infrared Detectors for Astronomy III, 70210P (24 July 2008);

- Hilbert, B., 2009, "'Snowballs' in the WFC3-IR Channel: Characterization," ISR WFC3 2009-43

- Hilbert, B., 2015, "NIRCam CV2 Testing: Snowball Census," Doc JWST-STScI-004407, SM-12

- McCullough, P. R., 2009, "Radioactivity in HgCdTe devices: potential source of 'snowballs'," ISR WFC3 2009-44

- Momcheva, I. et al., 2017, "A New Method for Wide-field Near-IR Imaging with the Hubble Space Telescope," PASP, 129, 5004

- Rauscher, B. J. et al., 2015, "New and Better Detectors for the JWST Near-Infrared Spectrograph," PASP, 126, 942

- Volk, K., 2014, "NIRISS/FGS Detector Selection: 'Snowball' Analysis," Doc JWST-STScI-003929, SM-12

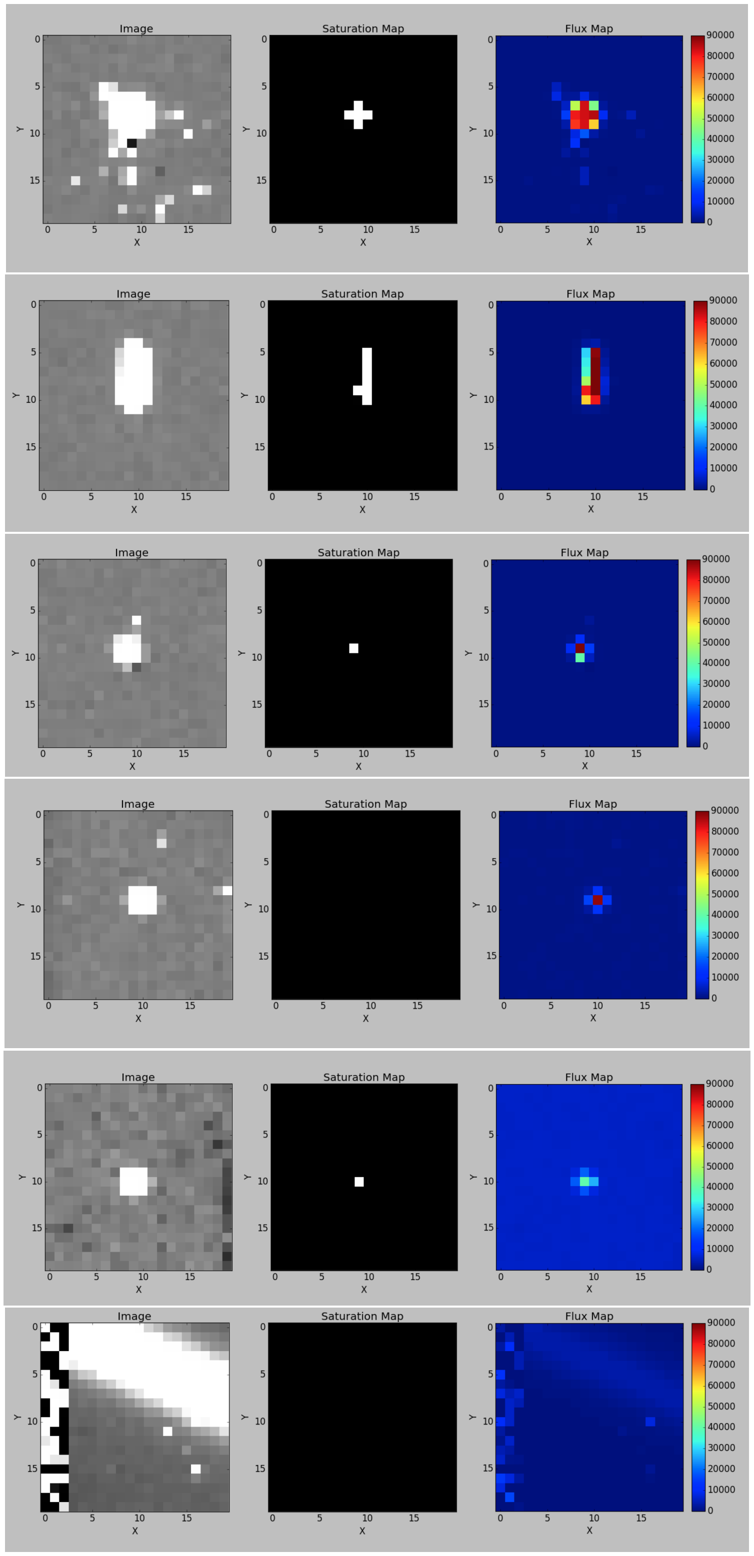

Figure 1: Six illustrative cases of snowball diagnostics. In each row, the first column shows a thumbnail image of the affected pixels sufficiently above background; the second column shows the saturated pixels; the third column shows an e^- flux map. We selected the top two cases as “candidate” snowballs, marked the middle two cases as “marginal” snowballs, and the bottom two were rejected.

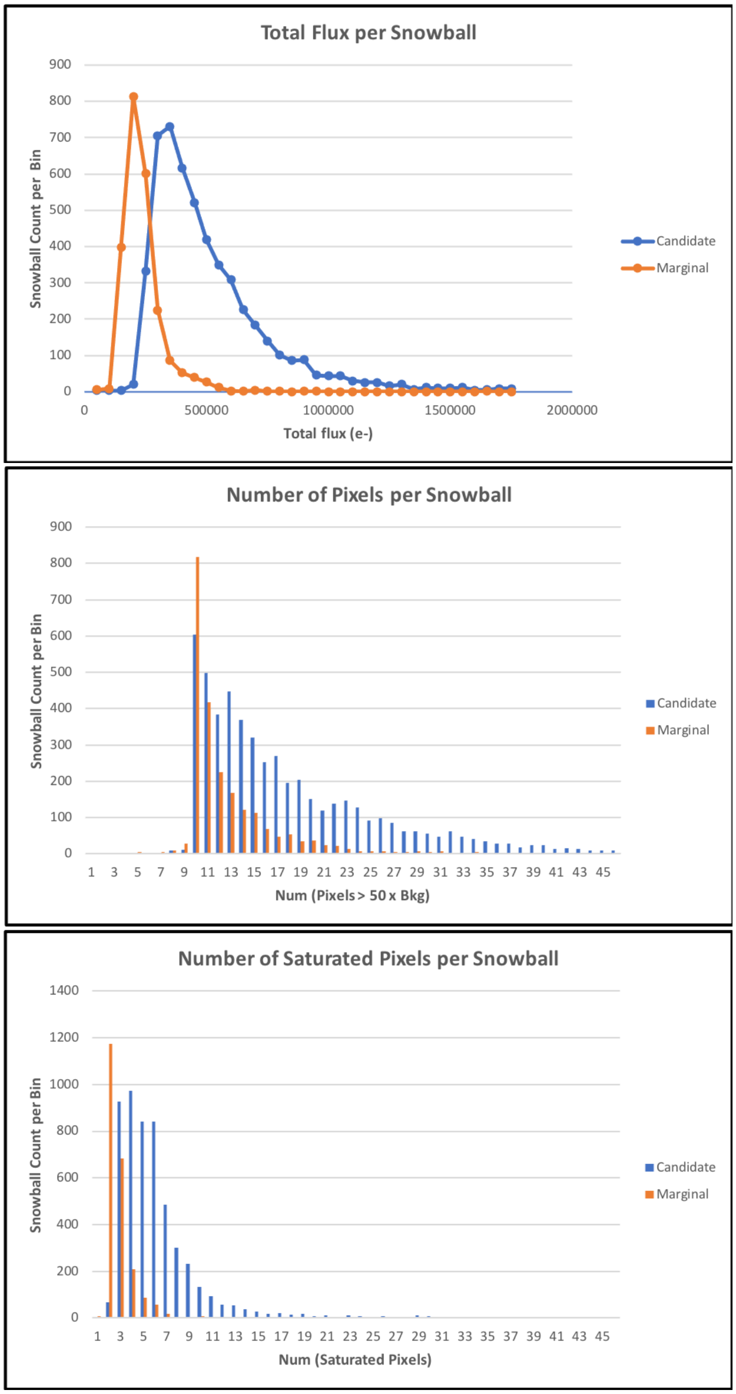

Figure 2: Number of snowballs as a function of: total flux (top), number of pixels with flux sufficiently above background (middle), and number of saturated pixels (bottom). In each chart, the blue points represent the count of "candidate" snowballs, and the orange lines represent the count of "marginal" snowballs in each bin.

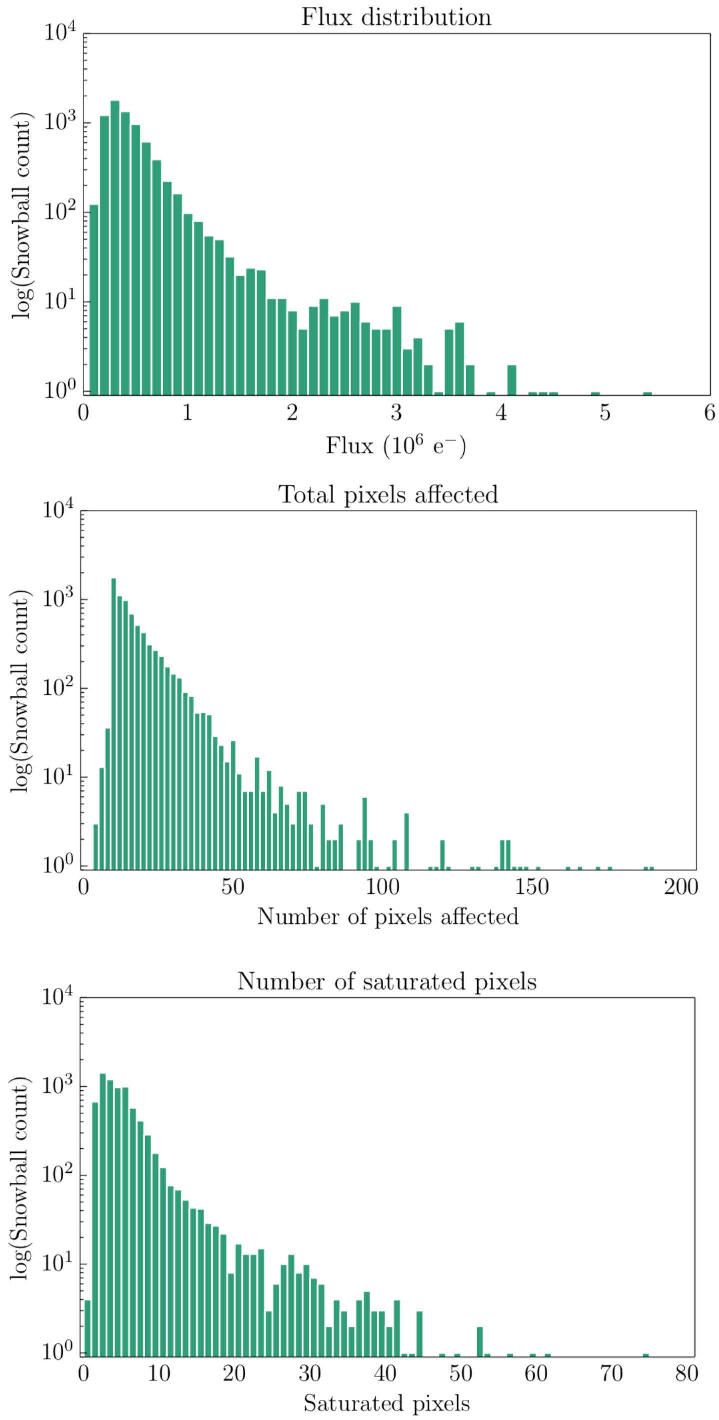

Figure 3: Number of snowballs a function of: total flux (top), number of pixels with flux sufficiently above background (middle), and number of saturated pixels (bottom), reproduced from D15 for the 2009-14 period.

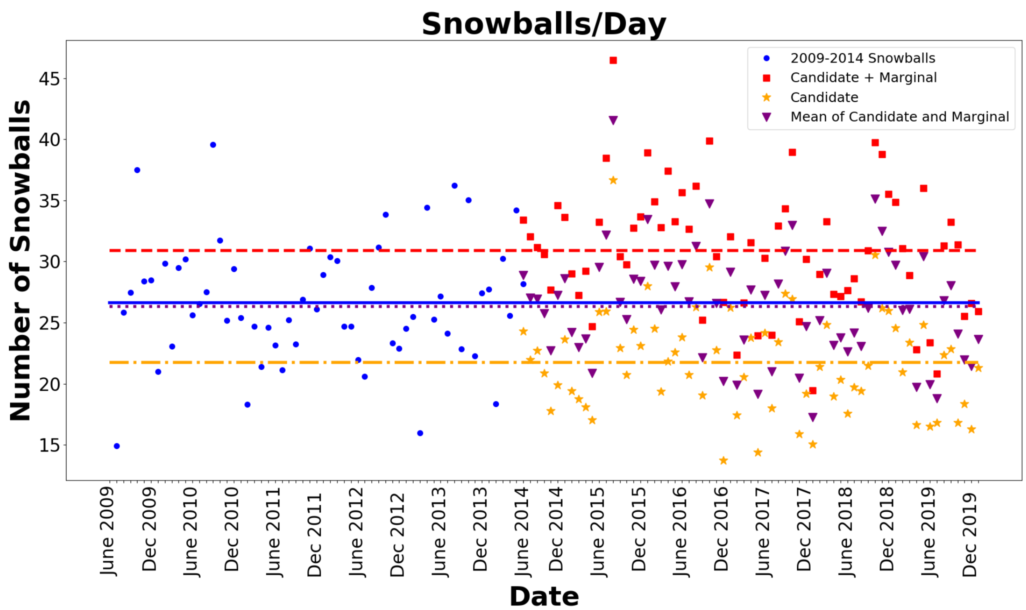

Figure 4: A comparison of the snowball normalized count from this work with the data in D15, per month from 2009 to present. The normalized snowball count per month from D15 is shown in blue circles and the monthly average as a solid blue line; the normalized "candidate" monthly snowball count from this work is shown in orange stars with the "candidate" monthly average as a dot-dashed orange line; the normalized total monthly snowball count from this work is shown in red squares with the total (candidate + marginal) monthly average as a dotted purple line. The D15 snowball rate average (a solid blue line, slightly offset from the dotted red line) falls midway between the average of "candidates" and total snowballs from this work(see text), highlighting the consistently measured rate despite differences between methods, and the lack of significant change in occurrence rate over time.

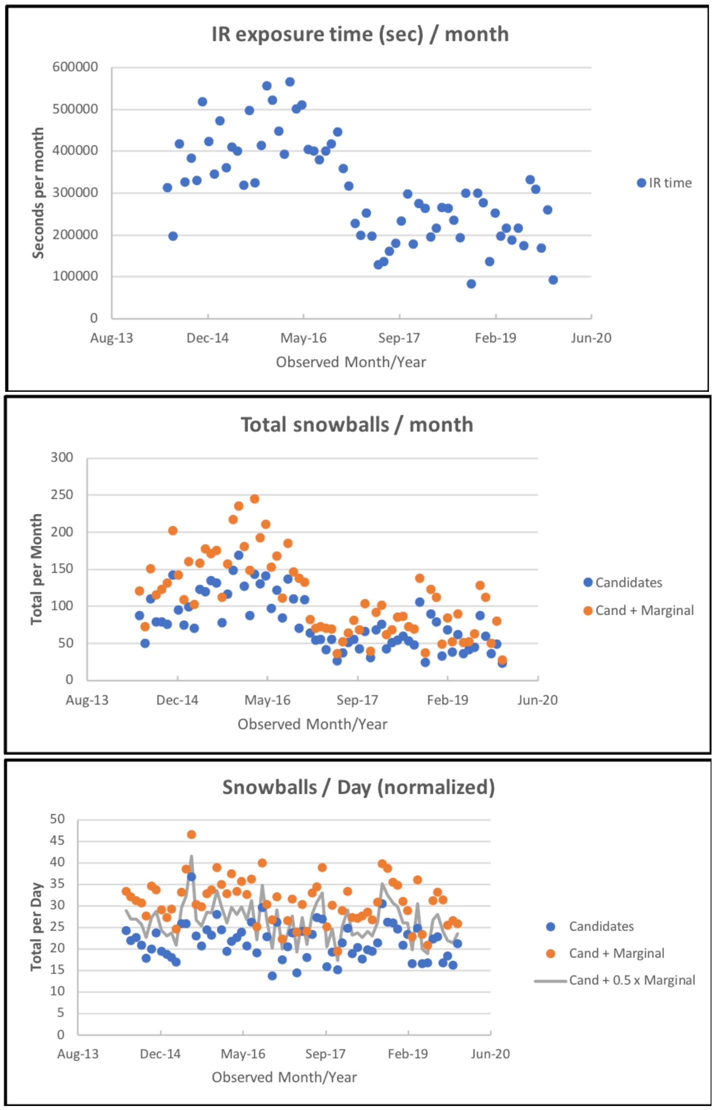

Figure 5: During each month from June 2014 to December 2019: total IR exposure time (top), total snowballs (middle), and normalized snowball count per day (bottom), showing the variance month-to-month. The bottom figure also includes a gray solid line indicating the count of candidates plus half of the marginal snowball detections per day.

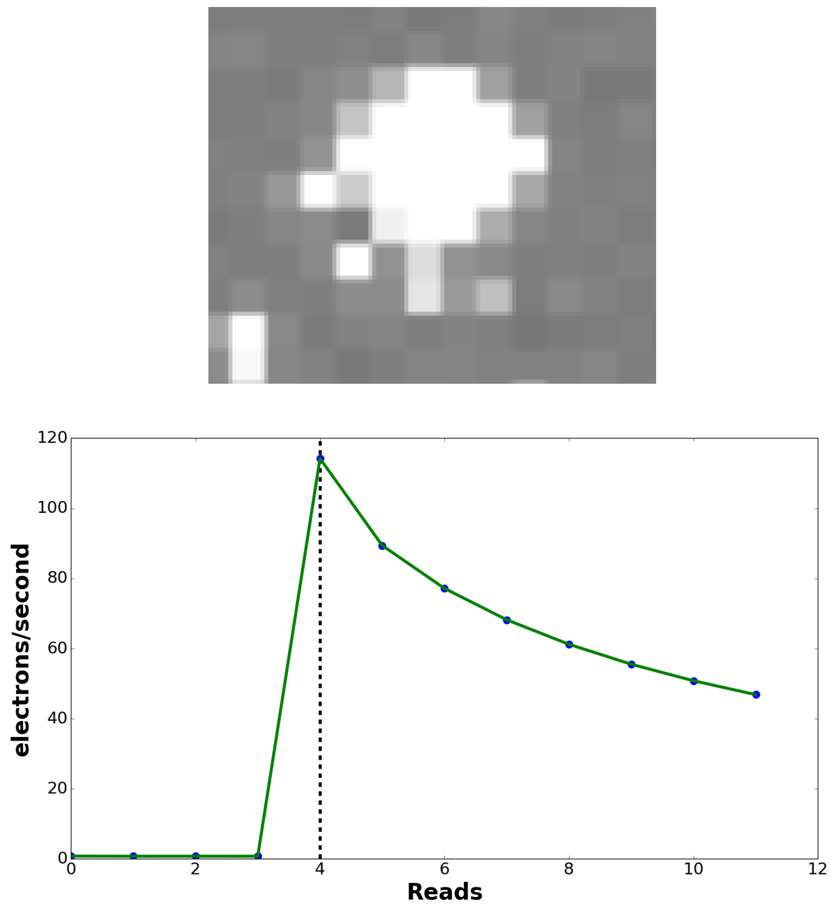

Figure 6: **Top:** An example case of a large, extended snowball canddiate. **Bottom:** The count rate in electrons per second of each read for the central 3×3 pixels, with the snowball occurring in read #4 (vertical dashed line).